

# RSC Advances

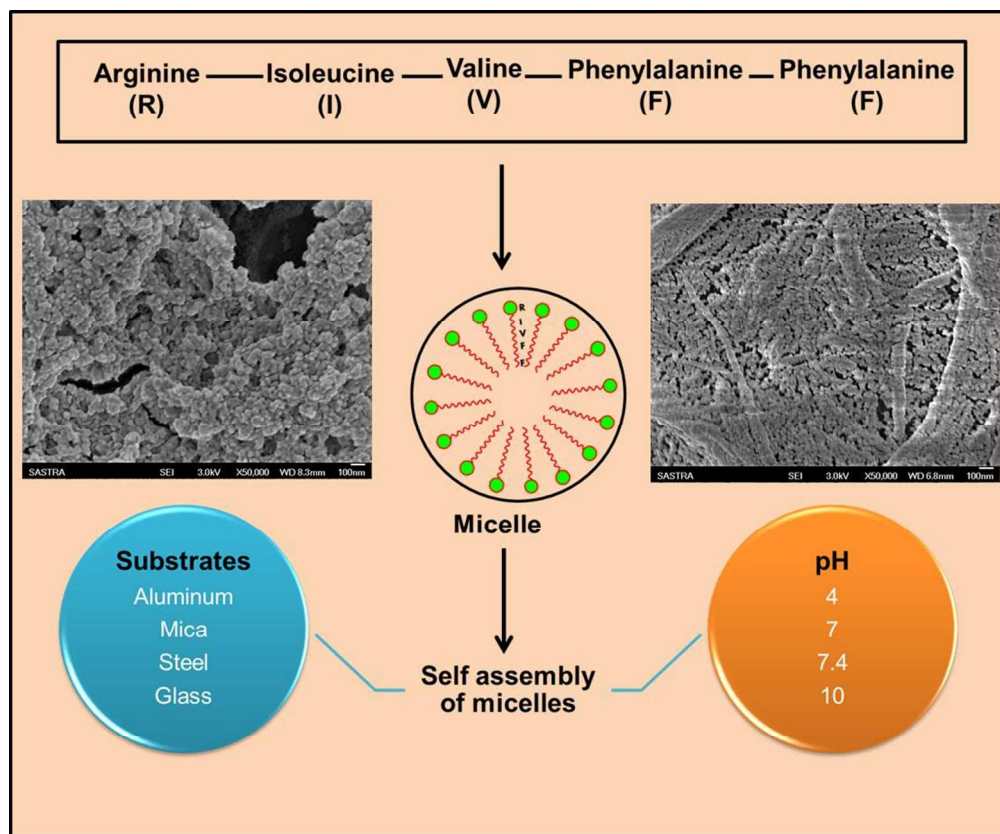


This is an *Accepted Manuscript*, which has been through the Royal Society of Chemistry peer review process and has been accepted for publication.

*Accepted Manuscripts* are published online shortly after acceptance, before technical editing, formatting and proof reading. Using this free service, authors can make their results available to the community, in citable form, before we publish the edited article. This *Accepted Manuscript* will be replaced by the edited, formatted and paginated article as soon as this is available.

You can find more information about *Accepted Manuscripts* in the [Information for Authors](#).

Please note that technical editing may introduce minor changes to the text and/or graphics, which may alter content. The journal's standard [Terms & Conditions](#) and the [Ethical guidelines](#) still apply. In no event shall the Royal Society of Chemistry be held responsible for any errors or omissions in this *Accepted Manuscript* or any consequences arising from the use of any information it contains.



188x155mm (150 x 150 DPI)

# Self-assembly characteristics of a structural analogue of *Tjernberg* peptide

Keerthana Ramaswamy, Priyadharshini Kumaraswamy, Swaminathan Sethuraman,  
Uma Maheswari Krishnan\*

Centre for Nanotechnology & Advanced Biomaterials  
School of Chemical & Biotechnology  
SASTRA University, Thanjavur 613401, Tamil Nadu, India

---

\*Corresponding Author

Prof. Uma Maheswari Krishnan Ph. D.  
Centre for Nanotechnology & Advanced Biomaterials  
School of Chemical & Biotechnology  
SASTRA University  
Thanjavur 613 401  
India.

Ph: +91 4362 264101 Ext 3677

Fax: +91 4362 264120

Email: [umakrishnan@sastra.edu](mailto:umakrishnan@sastra.edu)

**Abstract**

Molecular self-assembly of peptides have gained attention in the recent years due to the reproducibility of nanostructures that are formed with high degree of control over the kinetics of formation. These self-assembled nanostructures have been widely exploited for drug delivery, tissue engineering and also serve as a model system to understand the pathogenesis behind the protein misfolding diseases. In our study, an attempt has been made to understand the pathogenesis behind the formation of amyloid plaques using a modified version of KLVFF peptide. The self-assembly of RIVFF peptide was investigated in various substrates and in various pH. Our data revealed that the novel pentapeptide RIVFF self assembles into micelles of about 10 nm, which was confirmed by electron microscopy. The presence of hydrogen bonded beta sheet structures in the micelles were confirmed using FTIR, SAED, CD and thioflavin binding assay. The formation of higher order structures by the peptide in various pH and substrates was investigated using SEM. Finally the mode of action of the micelles formed by the peptide was confirmed by cytotoxicity studies in IMR-32 human neuroblastoma cell lines. The cytotoxicity of the nanostructures formed by the peptide may be attributed to the amino acids with long side chain along with hydrophobic amino acids resembling the cytotoxicity of amyloid beta peptide.

**Keywords:** Self-assembly, RIVFF, amyloid plaques, neuroblastoma

## Introduction

Molecular self-assembly systems lie at the interface between protein science, biochemistry, molecular engineering, polymer science and materials science. <sup>[1]</sup> Molecular self-assembly of biomolecules, especially peptides and proteins have generated immense interest in recent years due to the excellent reproducibility of the self-assembled structures and the high degree of control on the formation kinetics and morphology. <sup>[2]</sup> The rate of self-assembly and the type of self-assembled ensembles can be regulated by varying the self-assembly parameters. <sup>[3]</sup> Protein folding is a process of spontaneous molecular self-organization, by which protein structures attain their functional form. <sup>[4]</sup> Protein folding is a complex process, which is influenced by the solvent, concentration of salts, pH and temperature and thus it is extremely sensitive to extracellular milieu. Any change in the environmental parameters alters the native protein conformation resulting in protein misfolding that has been implicated in many neurodegenerative disorders. <sup>[5]</sup> In order to understand the factors influencing the folding (and misfolding) process as well as to decipher the mechanism of self-assembly leading to the formation of aggregates, many model systems have been designed and extensively investigated. <sup>[6]</sup> A plethora of self-assembled structures have been derived from peptides and these include micelles, <sup>[2]</sup> fibers, <sup>[7]</sup> tapes, <sup>[8]</sup> rods <sup>[9]</sup> and ribbons. <sup>[10]</sup> The nanostructures are relatively stable due to the lower Gibbs' free energy involved in the process. Peptide nanostructures have been explored for potential drug delivery applications <sup>[11]</sup> and electronic applications also. <sup>[12]</sup>

One of the widely investigated self-assembling systems is the aggregation of amyloid beta peptides that lead to formation of plaques in the brain leading to neurodegeneration.

<sup>[13]</sup> A large of body of literature exists on studies investigating the properties and functions of self-assembly process of amyloid beta peptides and analogues that contain recognition motifs similar to those present in amyloid beta. But their applications are not yet well developed using the self-assembled nanostructures due to the lack of understanding the mechanism of the process of self-assembly. It is reported that the order and directionality to the formation of amyloid structures are chiefly governed by aromatic and stacking interactions, which is also said to be the dominant factors involved in the formation of amyloid beta aggregates during the onset and progression of Alzheimer's disease. <sup>[14]</sup> The core-recognition motif namely KLVFF is reported to be responsible for the formation of beta structures by amyloid beta peptide. <sup>[15]</sup> These recognition motifs also undergo fibrillization like the amyloid beta peptide *via* formation of dimers, oligomers and protofibrils. <sup>[16]</sup>

Various characterization techniques like dynamic light scattering (DLS), Thioflavin T (ThT) fluorescence, surface plasmon resonance spectroscopy, atomic force spectroscopy, diffraction studies, electron microscopy, circular dichroism spectroscopy, Fourier transform infrared spectroscopy, gel electrophoresis, etc., have been widely employed to understand the kinetics involved in the self-assembly process and to extensively characterize the nanostructures formed. Recently, it was reported by our group that KLVFF forms micelles initially which then undergoes hydrogen bonding and stacking interactions to form higher order structures. <sup>[2]</sup> Various peptides derived from the KLVFF peptide has been reported to undergo self-assembly. Different parameters like solvent, stereochemistry, pH play an important role in determining the self-assembled structures formed by the peptide. For instance, AAKLVFF peptide is reported to form nanotubes in methanol and fibrils in water,  $\beta$ BAKLVFF peptide self-assembles to form twisted fibrils

and YYKLVFFC peptide transforms from nematic to isotropic phase on changing pH.<sup>[17]</sup> It was also reported by our group that the micelles formed by the KLVFF peptide have the ability to overcome the cytotoxicity caused by amyloid beta peptide and hence can be used for treatment of Alzheimer's disease.<sup>[2]</sup> A class of beta sheet blockers that includes KLVFF, also known as the Tjernberg peptide, has been defined as possible therapeutic moieties against Alzheimer's, though *in vivo* validation needs to be performed.

Understanding the key aspects in molecular self-assembly of the recognition motif of amyloid beta peptide can help to understand the pathogenesis caused by the self-assembly of amyloid beta peptide and to design the drug molecules to overcome the cytotoxicity caused by amyloid beta peptide. Various ultra small peptides that self-assemble to form cross beta sheet structure have been designed to understand the mechanism of amyloidogenesis. Results from the self-assembly studies of the ultra small peptides revealed that they form  $\alpha$ -helical intermediates before forming fibrils.<sup>[18]</sup> Thus understanding the process leading to the formation of fibrils is a key to design new therapeutic targets.

Based on the previous work on KLVFF by our group, a pentapeptide namely RIVFF has been designed that retained the dipeptide residue 'FF', which plays an important role in aromatic stacking interactions of the amyloid beta peptide. Since it is previously reported that charged amino acids possess the ability to disrupt amyloid plaques by means of electrostatic interactions, lysine residue in the Tjernberg peptide is replaced by a more cationic arginine. Amyloid beta peptide is found to localize itself by partially interacting with the lipid bilayer and hence it is reported that the custom made peptides with positively charged amino acids exhibit electrostatic interactions with the negatively charged phospholipids in the lipid bilayer and can either enhance or alleviate the toxic

effects of amyloid beta peptide.<sup>[19]</sup> The influence of a branched non-polar amino acid on the self-assembly was probed by replacing the leucine moiety in the Tjernberg peptide by isoleucine. Thus the sequence RIVFF is an analogue of the Tjernberg peptide KLVFF. This work investigates the self-assembly of the novel RIVFF peptide in various experimental conditions along with possible mechanism of action in presence of amyloid beta peptide.

## Results and Discussion

Figure 1 shows the HR-TEM image of the self-assembled structure formed by RIVFF peptide. Spherical structures of size 7-10 nm were observed. RIVFF peptide possesses an amphiphilic nature since it consists of a polar head group arginine followed by a hydrophobic segment consisting of isoleucine, valine and phenyl alanine. Due to its amphipathic character, it can spontaneously self assemble into micelles in aqueous media with the polar head facing the aqueous exterior and the hydrophobic acyl chain orients away from the aqueous milieu.

From the HR-TEM images it was observed that RIVFF forms spherical structures and in order to confirm that the spherical structures formed by RIVFF peptide are micelles, surface tension measurements were carried out with various concentrations of the peptide. Figure 2 shows the surface tension of water observed at various concentrations of the peptide. It was observed that the surface tension of the solvent is lowered significantly on addition of the peptide, which is a characteristic feature of micelle formation by amphiphiles. The Critical Micelle Concentration (CMC) is defined as the concentration of the surface-active agent above which micelle formation occurs



spontaneously.<sup>[20]</sup> Surface tension represents the contractive tendency of the surface of a liquid. It was observed that the addition of RIVFF reduces the surface tension of water suggesting that it can act as a surfactant similar to its analogue KLVFF.<sup>[21]</sup> On increasing the concentrations of RIVFF, the surface tension decreases steeply and then plateaus off. Beyond a peptide concentration of 0.12 mg/mL, the surface tension exhibits another sharp decrease. These three distinct regions represent formation of a monolayer by the peptide amphiphile and finally the formation of micelle. From the surface tension versus concentration plot, the critical micelle concentration (CMC) of the peptide was found to be 0.12 mg/mL (Figure 2).

Selected Area Electron Diffraction (SAED) pattern obtained from the micellar aggregates of RIVFF peptide showed periodicities at 4.7 Å and 9.1 Å (Figure 3). While the periodicity of 4.7 Å has been attributed to the meridional diffraction of  $\beta$  sheet structures,<sup>[21]</sup> the periodicities at 9.1 Å have been assigned for equatorial diffraction of  $\beta$  sheet structures.<sup>[21]</sup> This indicates that the self-assembled structures formed from RIVFF comprise of predominantly beta sheets. This is similar to the KLVFF peptide, an analogous pentapeptide that has been reported to spontaneously self-assemble in to beta sheets.<sup>[7]</sup>

The micellar assemblies were characterized for the presence of hydrogen bonds by FT-IR spectroscopy using Attenuated Total Reflectance (ATR) mode (Figure 4). The band at 1637  $\text{cm}^{-1}$  shows the presence of amide I band, which suggests the presence of hydrogen bonded beta sheet in RIVFF at the concentration of 0.2 mg/mL. The vibration band between 3300  $\text{cm}^{-1}$  and 3500  $\text{cm}^{-1}$  may be attributed to aliphatic N-H stretch and O-H stretch.<sup>[22]</sup> The band at 1086  $\text{cm}^{-1}$  may be attributed to the primary amine C-N stretch.<sup>[22]</sup>

The vibration bands at  $985\text{ cm}^{-1}$ ,  $868\text{ cm}^{-1}$  and  $531\text{ cm}^{-1}$  correspond to aromatic C-H out of plane bend. <sup>[22]</sup>

Thioflavin T (ThT) binding assay was carried out to identify the presence of beta sheet structures in the peptide. Thioflavin T, a cationic benzothiazole dye shows an enhanced fluorescence upon binding to amyloid beta sheet structures and hence is commonly employed to diagnose amyloid fibrils in both *in vitro* and *in vivo*. <sup>[23]</sup> When ThT was incubated with the RIVFF peptide, its excitation and the emission wavelength was shifted to 440 nm and 490 nm respectively. The red shift in the excitation and emission indicates binding to beta sheet structures. Figure 5 shows a time dependent increase in the fluorescence emission intensity of thioflavin T (Th T) on incubation with RIVFF peptide. This suggests the existence of beta sheet structures formed by the peptide and this aggregation increases progressively with time.

To further understand the influence of pH on the secondary structures of the peptide, circular dichroism studies were carried out (Table 1). It was observed that the content of alpha helix, beta sheets and turns is influenced by the pH of the medium. The maximum amount of beta sheets was observed in deionized water. In the presence of ions, the beta sheet content reduces by nearly 57% at pH 4 and 7.4. Interestingly, when the pH approaches the isoelectric point of RIVFF (pI 10.3), the beta sheet content approaches closer to that observed in the absence of ions. It was implicit that the charge status of the peptide influences the aggregation. <sup>[24]</sup> The zwitter-ionic form of the peptide is significant both in the absence of ions as well at pH closer to its isoelectric point. This might lead to greater associative forces between the peptide chains leading to the formation of aggregates. At pH well below the isoelectric point of the peptide, it will possess a positive charge that will introduce repulsive forces between the polymer chain. The CD

results suggest that the propensity to exist in non-beta sheet forms is higher at pH 4 and 7.4. Even in the absence of ions, the maximum beta sheet content is less than 45%, which is much lower than that observed for its analogue KLVFF (unpublished data). The reduced tendency to form  $\beta$ -sheets by RIVFF may be due to presence of branched isoleucine moiety that may hinder close association of the peptide chains to form  $\beta$ -sheets. Instead, the propensity to form alpha helices and random coils is high due to the presence of the bulky side groups in isoleucine and arginine. Supplementary Figure 1 shows the CD spectrum for RIVFF peptide at various pH.

Figures 6A and 6B show the absorption and emission spectra of RIVFF peptide obtained using UV-Visible spectrophotometry and fluorescence spectroscopy respectively. The peptide shows an absorption maxima at 257 nm and a fluorescence emission at 290 nm when excited at 257 nm. The presence of the emission band at 290 nm indicates the possibilities of  $\pi$ - $\pi$  stacking interactions between the aromatic amino acids in RIVFF.<sup>[2]</sup> These interactions in turn may help in the stabilization of higher ordered structures formed by the peptide.

The spontaneous self-assembly of a peptide is influenced by numerous factors that include the nature and texture of the substrate, its hydrophobicity, surface tension, pH of the medium, temperature, ions and molecules in the medium and the concentration of the peptide.<sup>[2]</sup> This information can help to understand the nature of self-assembled structures that can be formed by the peptide in the *in vivo* conditions.

The influence of substrate-driven factors and pH on the self-assembly of RIVFF was investigated. Figure 7 shows the scanning electron micrographs of the self-assembled structures formed on four different substrates namely stainless steel, mica, aluminum and glass at different pH. From the scanning electron micrographs, micellar structures are

clearly discernible on all substrates at pH 4 and pH 7. These micellar structures exhibit a tendency to associate to form ordered arrays of micelles leading to fibrillar networks at higher pH that are more prominent in glass, stainless steel and mica. The peptide forms forests of short fibrils on aluminum substrate at pH 10. These differences may arise due to differences in the hydrophobicity and surface charge of the substrates. All the four substrates are hydrophilic with contact angle less than 60°. However the hydrophilicity decreases in the order: Mica (13°) > Glass (33°) > Stainless steel (45°) > Aluminum (53°). Aluminum displays the least hydrophilicity among the four substrates investigated and this might have contributed to the differences in the self-assembled structures formed in aluminum when compared with the other substrates.

The hydrophilicity of the substrate might also exert an influence on the rate of solvent evaporation from the peptide that may influence the self-assembled structures formed. The net surface charge on these surfaces may also influence the nature of self-assembled structures. While aluminum, glass and mica are negatively charged, stainless steel is positively charged. As RIVFF has a positive charge due to the presence of arginine moiety, it is expected to exhibit electrostatic interaction with the negatively charged surface of aluminum, mica and glass. Hence well spread aggregates were observed on these surfaces. The stainless steel surface is expected to repel the RIVFF head group and hence it is possible that a vertical stacking may be preferred by the peptide to reduce the repulsive forces. The presence of aromatic phenylalanine moieties may result in  $\pi$ - $\pi$  stacking interactions that may contribute to the vertical stacking. The formation of micelle by RIVFF on all substrates is expected owing to the strong amphiphile nature of the peptide. The presence of short fibrils in mica substrate may be influenced by the

substrate topography that is rough leading to more vertical stacking. Glass and aluminum foil are smooth and hence exhibit better spreading of the self-assembled structures.

### **Influence of pH**

It was observed that micelle structures were found on all substrate at all pH (4, 7, 7.4 and 10). However, as the pH increases, larger aggregates were observed suggesting a reduction in the repulsive force between the peptide chains. This is because the isoelectric point of RIVFF is 10.3 and the increase in pH reduces the positive charge in the peptide. Higher pH tends to promote greater peptide-peptide interaction than substrate-peptide interaction.

The Tjernberg peptide, which is a structural analogue of KLVFF has been found to mitigate the toxic effects of amyloid beta plaques using different models. In an attempt to evaluate the potential of RIVFF to reverse amyloid induced toxicity in cells, *in vitro* studies were carried out using IMR 32 cells. Figure 8 shows the viability of IMR 32 cells exposed to different concentrations of RIVFF in the presence of amyloid beta peptide. It was observed that the presence of 10  $\mu$ M amyloid beta peptide reduces the cell proliferation by 70 % when compared with the negative control confirming the toxic nature of A $\beta$ . On introduction of RIVFF to the system containing A $\beta$ , no significant improvement was observed in the cell viability. Instead, as the concentration of RIVFF was increased, the cell viability slightly decreases clearly indicating that RIVFF does not possess  $\beta$ -sheet breaking ability unlike its structural analogue KLVFF. Instead its propensity to form micelles accelerates the binding and anchoring of the A $\beta$  to the membrane surface thereby augmenting the cytotoxic effects of A $\beta$ . In order to know whether RIVFF at high concentrations were toxic, cell viability studies has been carried out with various concentrations of RIVFF in the absence of A $\beta$ . Supplementary Figure 2

shows that the cell viability is not altered at low concentrations of RIVFF (50  $\mu\text{M}$  and 100  $\mu\text{M}$ ). However at high concentrations (250  $\mu\text{M}$  and 500  $\mu\text{M}$ ), RIVFF peptide is found to be cytotoxic. Hence it is confirmed that the reduction in cell viability at 1:25 and 1:50 ratio of  $\text{A}\beta$ : RIVFF is attributed to the fibrillar structures formed by RIVFF peptide. The difference between RIVFF and KLVFF in ameliorating the  $\text{A}\beta$ -induced toxicity may be due to their different abilities to reduce surface tension. Reduction in surface tension is considered an important factor in binding of the peptide to the core recognition motif of  $\text{A}\beta$  and disrupts the beta sheet structures formed by it. RIVFF, due to its lower surface tension may not serve as an effective chaotropic agent. In addition, the highly cationic peptide could also exhibit toxic effects to cells. Thus, it appears that RIVFF behaves more as an  $\text{A}\beta$  analogue and does not possess therapeutic effects. However, its ability to reduce cell viability may be explored in future as a possible cytotoxic agent.

## **Materials and Methods**

### **Materials**

The peptide sequence with 95% purity was procured from M/s Gray Matter Research Foundation Private Limited, Trichy. Fresh peptide stock solution was prepared by dissolving the lyophilized peptide in 1,1,1,3,3,3-hexafluoro-2-propanol (HFIP),  $(\text{CF}_3)_2\text{CHOH}$  purchased from Sigma Aldrich, USA. Millipore water and double distilled water were used for all the experiments.

### **Preparation of Sample**

RIVFF peptide stock was prepared by dissolving the peptide with HFIP at a concentration of 2 mg/mL to remove any aggregates. To avoid pre-aggregation, fresh

stock was prepared for each experiment. HFIP is a polar solvent, which exhibits strong hydrogen bond and thus it has the ability to dissolve the peptide and form homogenous solution. It was then evaporated in vacuum and diluted to the desired concentration using sterile deionised water freshly before use.

For self-assembly studies, samples were prepared by diluting the peptide stock solution with de-ionized water to a final concentration of 0.2 mg/mL. Ten micro liters of the sample was then placed on the substrate (aluminum, glass, stainless steel or mica) and subsequently dried in vacuum for 12 hours. The influence of pH on the self-assembly was carried out using 0.1 M acetate buffer (for pH 4) and 0.1 M phosphate buffer (for pH 10) and PBS (for pH 7.4).

### **Characterization Techniques**

Self-assembled structures formed by the peptide were analyzed using Field Emission Scanning Electron Microscopy (FE-SEM) (JSM 6701F Japan) and Transmission Electron Microscopy (FE-TEM) (JEM 2100F, JEOL, Japan).<sup>[7]</sup> For TEM analysis, the sample was prepared by diluting the stock solution to 0.2 mg/mL using de-ionized water. It was then placed in a TEM grid and kept in vacuum until drying. Then the sample was imaged without further staining using Field emission Transmission electron microscope (JEM 2100F, JEOL, Japan). For selected area electron diffraction studies, TEM mode was changed to diffraction mode and image was recorded for the micelles. Morphological analysis of self-assembled nanostructures was carried out using field emission scanning electron microscopy. Briefly, the samples were placed on a brass stub using double-sided carbon tape and a thin film of gold was coated using sputter coating at a current of 20 mA for 45 s. The sputter-coated samples were then introduced into the specimen chamber and imaging was carried out at an accelerating voltage of 3 kV. To determine the formation of

micelles in aqueous solvents, the stock solution was diluted to 0.2 mg/mL using deionised water and freeze-dried for about 48 hours. The powder obtained was then imaged after gold coating using the procedure mentioned above. Presence of hydrogen bonded beta sheet structures was confirmed using Fourier Transform Infrared Spectroscopy (FTIR) (Spectrum 100, Perkin Elmer, USA).<sup>[7]</sup> The spectrum of the peptide was recorded in the Attenuated Total Reflection (ATR-FTIR) mode between 4000 and 400  $\text{cm}^{-1}$  at a resolution of 4  $\text{cm}^{-1}$  averaging 20 scans per sample. The stock solution was diluted to 0.2 mg/mL using distilled water and the spectrum was recorded. Absorption spectra were measured by using UV-visible spectrophotometry (Lambda 25, Perkin Elmer, USA).<sup>[2]</sup> Samples were prepared by diluting the stock solution in double distilled water and scanned between 200– 800 nm to determine the absorption maxima of the RIVFF peptide. For determining critical micelle concentration, different concentrations of the peptide was prepared in phosphate buffered saline (PBS) and scanned between 200 and 800 nm. The absorbance maximum at 257 nm was plotted against the concentration. Fluorescence spectra were recorded by spectrofluorimetry (LS 45, Perkin Elmer, USA).<sup>[2]</sup> Samples were prepared by diluting the stock solution in deionised water and scanned for emission from 260–400 nm by using the excitation wavelength of 257 nm, which was obtained from UV-visible spectrophotometer. Surface tension measurements were carried out using Goniometer (250 F1, Rame-Hart, USA). Briefly different concentrations (0.02, 0.04, 0.06, 0.08, 0.1, 0.12, 0.14, 0.16, 0.18, and 0.2 mg/mL) of the samples were prepared and a drop was formed in the needle tip (gauge size 24G). The sample droplet was focused using CCD camera and surface tension measurements were made using pendant drop method software available with the instrument. The experiment was performed three times and the average surface tension was calculated and plotted against concentration.



Circular Dichroism (CD) spectroscopy was performed at room temperature for RIVFF over a wavelength range of 190-260 nm (JASCO 810, Spectropolarimeter, USA). A quartz cell with 5 mm path length was used for recording the CD spectra of the peptide sample with a concentration of 25  $\mu\text{g/mL}$ . The spectra were obtained at different pH of 4, 7, 7.4 and 10 with a bandwidth of 1 nm averaging 4 scans per sample. The secondary structures were calculated using the software available with the instrument.

### **Thioflavin T Binding Assay (ThT)**

The stock solution was prepared by dissolving 3 mg of Thioflavin T (ThT) in 1 mL of double distilled water and the solution was filtered through a 0.2 mm syringe filter. The concentration of Thioflavin T was calculated from the absorbance measured at 416 nm. A 1 mM ThT solution and 0.2 mg /mL peptide sample was used for the assay. At various time points, the emission intensity was measured at 490 nm corresponding to an excitation wavelength of 450 nm.

### **Cell culture and cell seeding**

IMR 32 human neuroblastoma cells (NCCS, Pune) were cultured in Dulbecco's Modified Eagle Medium (DMEM, Gibco, USA) supplemented with 10% Fetal Bovine Serum (FBS, Gibco, USA) and 1% penicillin/streptomycin. The culture was then maintained at 37°C in 5% carbon dioxide in an incubator. About ten thousand cells were seeded in a 96 well plate and the cells were incubated with 10  $\mu\text{M}$  amyloid beta peptide ( $\text{A}\beta$  1–42) solution 48 hours after seeding. After 48 hours of incubation, different concentrations of RIVFF peptide solution (100  $\mu\text{M}$ , 250  $\mu\text{M}$  and 500  $\mu\text{M}$ ) were added to it such that the ratio of  $\text{A}\beta$  to RIVFF was 1: 10, 1: 25 and 1: 50.

### **Cell Cytotoxicity**

Cytotoxicity was evaluated using the 3-(4,5-dimethylthiazol-2-yl)-5-(3-carboxymethoxyphenyl)-2-(4-sulfophenyl)-2H-tetrazolium (MTS) assay. Cells were incubated with 10  $\mu$ M amyloid beta peptide (A $\beta$  1–42) for 24 hours followed by another 48 hours of incubation with RIVFF. The media was then removed and the cells were washed with phosphate buffered saline (PBS) to remove any non-adherent cells. 200  $\mu$ L of serum free media and 20  $\mu$ L of MTS reagent was added and incubated at 37°C for 2 hours. The reaction was stopped by the addition of 250  $\mu$ L of 10% sodium dodecyl sulfate (SDS) solution and the absorbance was then measured at 490 nm using a multimode reader (Infinite 200M, Tecan, USA). Cells incubated with 10  $\mu$ M amyloid beta peptide (A $\beta$  1–42) served as positive control while cells without amyloid beta peptide (A $\beta$  1–42) served as negative control.

### Conclusion

Many reports have shown that KLVFF has been used to block the aggregation of the amyloid beta fibrils through intercalation between two amyloid beta molecules. Based on the KLVFF motif, an analogue RIVFF has been designed and its self-assembly characteristics were investigated. Our data shows that the novel peptide formed micelles that then associated to form higher order structures. Self-assembly has been investigated on various substrates and pH. An increase in the dimension of the nanostructure was observed with increasing pH. The hydrophobicity, charge and topography of the substrate were found to influence the nature of the self-assembled structures formed. The tendency to form  $\beta$ -sheets is not very high in RIVFF due to the presence of the branched amino acid isoleucine. *In vitro* studies revealed that the presence of branched amino acid might be a major contributor to the accelerated loss in cell viability observed in the presence of amyloid beta. The micellar structures may promote binding of the A $\beta$  on the membrane

surface causing cytotoxicity and hence this peptide could have applications as an A $\beta$  analogue or as a cytotoxic agent rather than a beta-blocker like its analogue Tjernberg peptide, KLVFF.

### Acknowledgement

The authors wish to acknowledge SASTRA University and PG Teaching Programme (No. SR/NM/PG-16/2007) of the Nano Mission Council, Department of Science & Technology, New Delhi for the infrastructural support. The second author P.K wishes to thank Department of Science & Technology for the INSPIRE Fellowship grant (DST/INSPIRE Fellowship/2011/74). We also thank Madurai Kamaraj University for CD measurements.

### References

1. X. Zhao and S. Zhang, *Chem. Soc. Rev.*, 2006, **35**, 1105-1110.
2. P. Kumaraswamy, S. Sethuraman and U.M. Krishnan, *Soft Matter*, 2013, **9**, 2684-2694.
3. G.M. Whitesides, J.K. Kriebel and B.T. Mayers, *Nanoscale assembly. Nanostructure Science and Technology* 2005, 217-239.
4. A.M. Lesk and G.D. Rose, *Proc. Natl. Acad. Sci. U.S.A.*, 1981, **78**, 4304-4308.
5. J.K. Weber and V.S. Pande, *Biophys. J.*, 2012, **102**, 859-867.
6. E. Gazit, *Prion*, 2007, **1**, 32-35.
7. P. Kumaraswamy, R. Lakshmanan, S. Sethuraman and U.M. Krishnan, *Soft matter*, 2011, **7**, 2744-2754.
8. A. Aggeli, G. Fytas, D. Vlassopoulos, T.C. McLeish, P.J. Mawer and N. Boden, *Biomacromolecules*, 2001, **2**, 378-388.

9. S. Maity, P. Jana, S.K. Maity and D. Halder, *Langmuir*, 2011, **27**, 3835-3841.
10. E. Kokkoli, A. Mardilovich, A. Wedekind, E.M. Rexeisen, A. Garg and J.A. Craig, *Soft matter*, 2006, **2**, 1015-1024.
11. A. Altunbas, S.J. Lee, S.A. Rajasekaran, J.P. Schneider and D.J. Pochan, *Biomaterials*, 2011, **32**, 5906-5914.
12. S. Scanlon and A. Aggeli, *Nanotoday* 2008, **3**, 22-30.
13. C.A.E. Hauser, R. Deng, A. Mishra, Y. Loo, U. Khoe, F. Zhuang, D.W. Cheong, A. Accardo, M.B. Sullivan, C. Riekel, J.Y. Ying and U.A. Hauser, *Proc. Natl. Acad. Sci.*, 2011, **108**, 1361-1366.
14. E. Gazit, *FASEB J.*, 2002, **16**, 77-83.
15. P. Kumaraswamy, S. Sethuraman and U.M. Krishnan, *J. Agric. Food Chem.*, 2013, **61**, 3278-3285.
16. I. Khetarpal, M. Chen, K.D. Cook and R. Wetzel, *J. Mol. Biol.*, 2006, **361**, 785-795.
17. I.W. Hamley, V. Castelletto, C. Moulton, D. Myatt, G. Siligardi, C.L.P. Oliveria, J.S. Pederson, I. Abutbul and D. Danino, *Macromol. Biosci.*, 2010, **10**, 40-48.
18. A. Lakshmanan, D.W. Cheong, A. Accardo, E. Di Fabrizio, C. Riekel and C.A.E. Hauser, *Proc. Natl. Acad. Sci.*, 2012, **110**, 519-524.
19. K. Tao, J. Wang, P. Zhou, C. Wang, H. Xu, X. Zhao and J.R. Lu, *Langmuir*, 2011.
20. H. Iyota and R. Krastev, *Colloid Polym. Sci.*, 2009, **287**, 425-233.
21. T.R. Jahn, O.S. Makin, K.L. Morris, K.E. Marshall, P. Tian, P. Sikorski and L.C. Serpell, *J. Mol. Biol.*, 2010, **395**, 717-727.
22. J. Coates in *Encyclopedia of Analytical Chemistry*, ed. R.A. Meyers, John Wiley & Sons, Chicester, 2000, pp. 10815-10837.

23. H. Naiki, K. Higuchi, M. Hosokawa and T. Takeda, *Anal. Biochem.*, 1989, **177**, 244-249.

24. J.A. Loureiro, S. Rocha and C. Pereira Mdo, *J. Pept. Sci.*, 2013, **19**, 581-587.

### Table & Figures Legends

**Table 1:** Percentage of different secondary structures of RIVFF at various pH

**Figure 1:** HR-TEM image of RIVFF self-assembled spherical structures

**Figure 2:** Surface tension of RIVFF peptide at various concentrations

**Figure 3:** Selected Area Electron Diffraction image of micellar aggregates formed by RIVFF peptide

**Figure 4:** FTIR spectrum of RIVFF using Attenuated Total Reflectance (ATR mode)

**Figure 5:** Time dependent Thioflavin T (ThT binding assay) using fluorescence spectroscopy

**Figure 6:** [A] Absorption and [B] emission spectra of RIVFF peptide obtained using UV-Visible spectrophotometry and fluorescence spectroscopy respectively

**Figure 7:** Scanning electron micrographs of self-assembled structure formed by RIVFF on various substrates namely stainless steel, mica, aluminum and glass at different pH

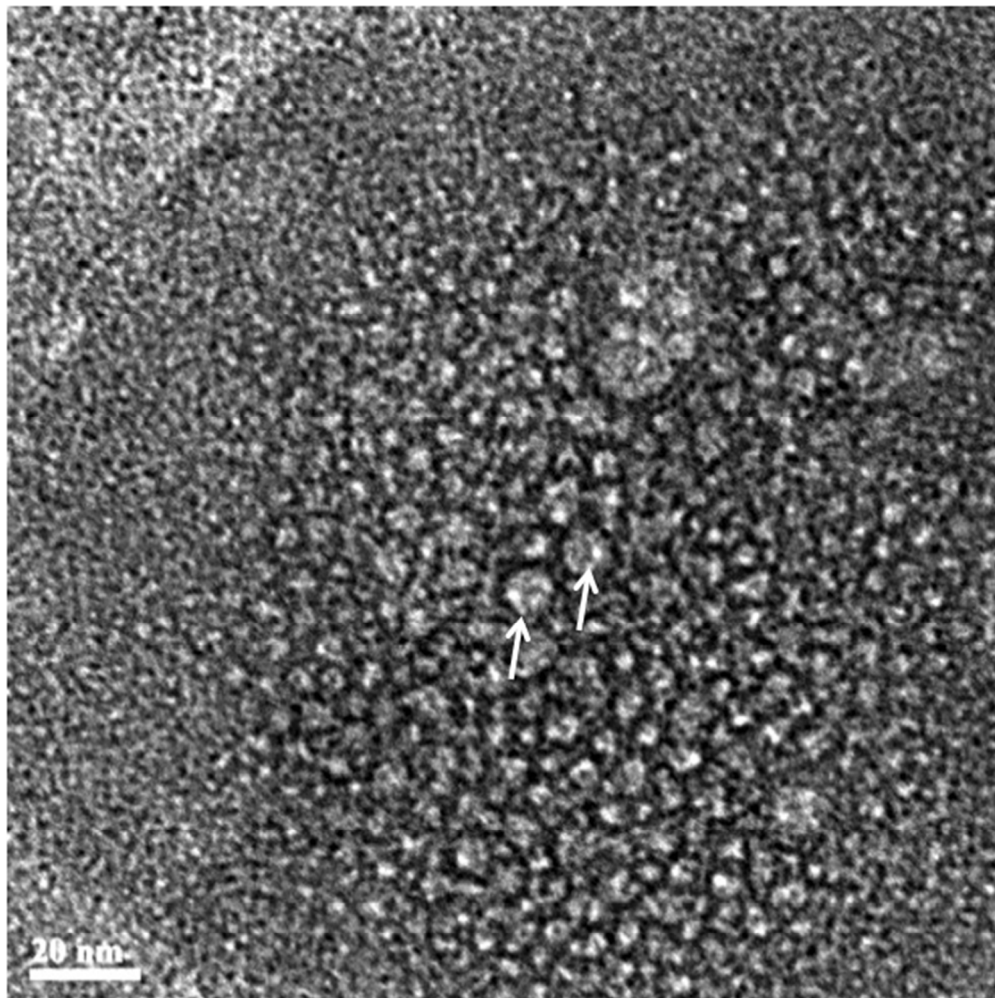
**Figure 8:** Cell viability of neuroblastoma cells exposed to different concentration of peptide in the presence of A $\beta$ <sub>1-42</sub>

**Supplementary Figure 1:** CD spectrum for RIVFF peptide at various pH.

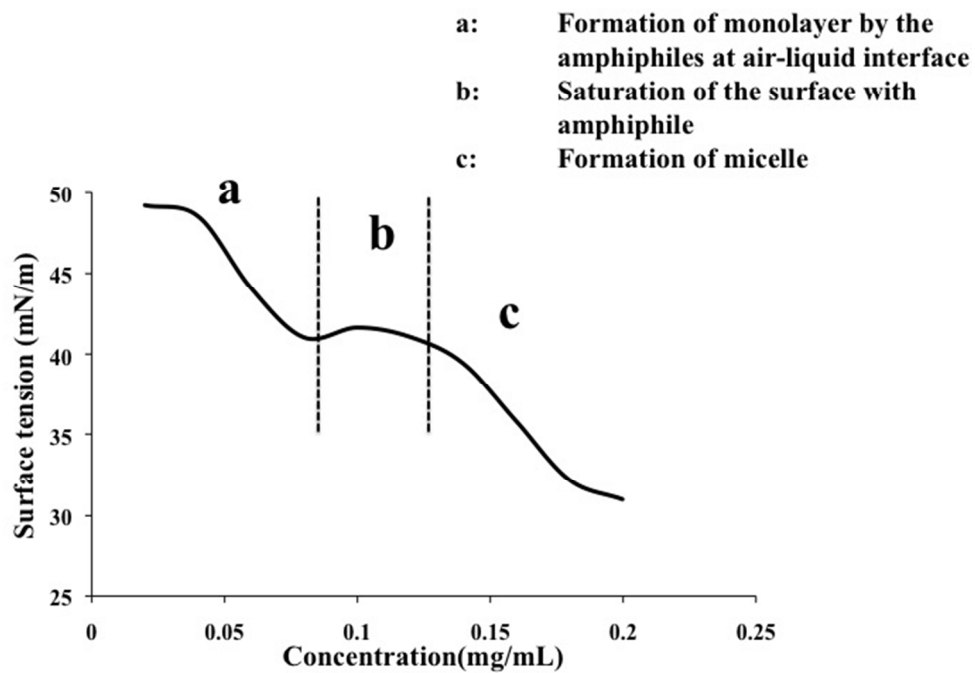
**Supplementary Figure 2:** Cell viability of neuroblastoma cells exposed to different concentration of peptide in the absence of A $\beta$ <sub>1-42</sub>

**Table 1.**

<b>pH</b>	<b>Alpha helix</b>	<b>Beta sheet</b>	<b>Turn</b>	<b>Random coil</b>
4.0	25.5	18.3	20.7	35.5
7.0	18.8	42.3	12.9	26.0
7.4	27.4	17.6	23.2	31.8
10.0	16.7	35.6	20.2	27.5

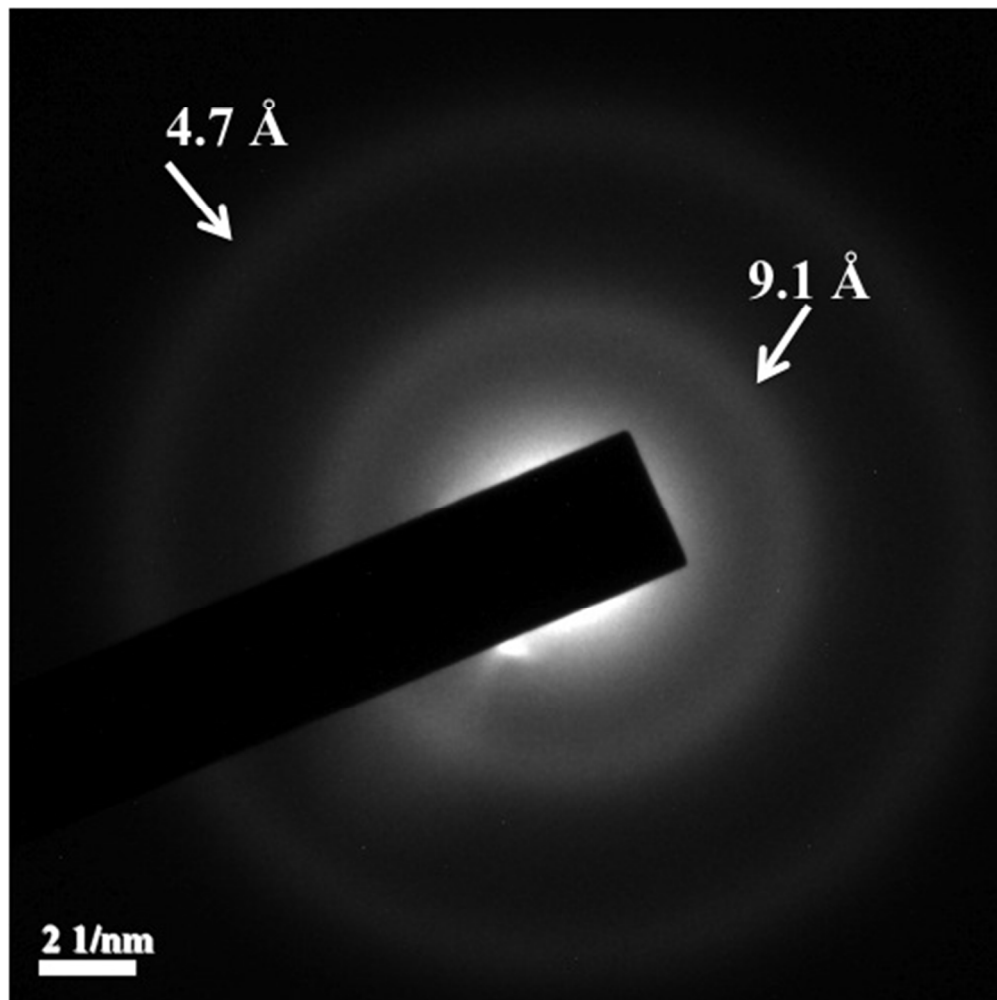


HR-TEM image of RIVFF self-assembled spherical structures  
218x224mm (72 x 72 DPI)

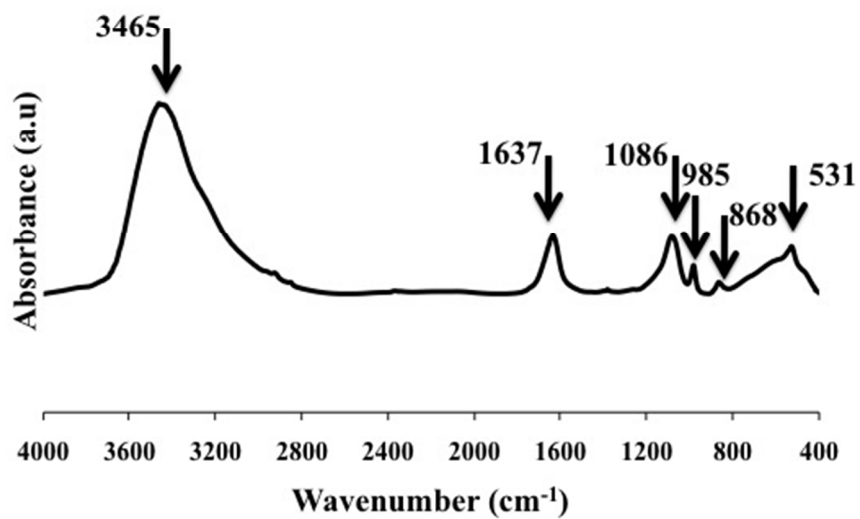


Surface tension of RIVFF peptide at various concentrations  
250x169mm (72 x 72 DPI)

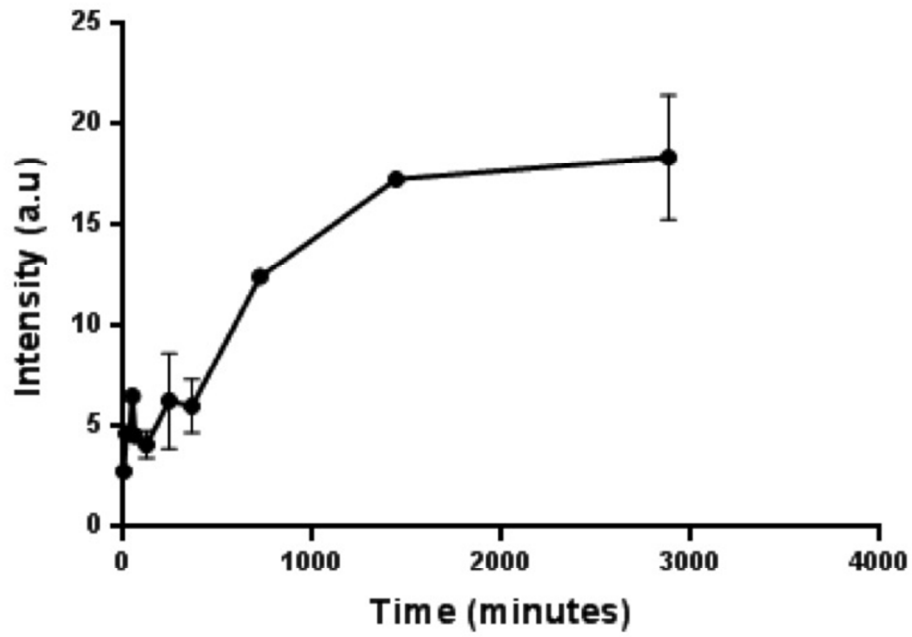




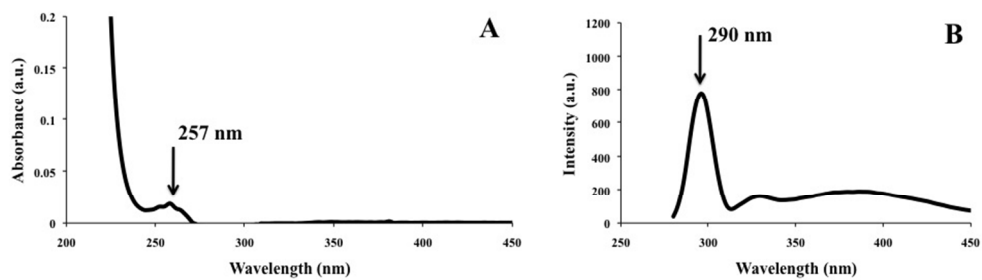
Selected Area Electron Diffraction image of micellar aggregates formed by RIVFF peptide  
178x178mm (72 x 72 DPI)



FTIR spectrum of RIVFF using Attenuated Total Reflectance (ATR mode)  
216x154mm (72 x 72 DPI)



Time dependent Thioflavin T (ThT binding assay) using fluorescence spectroscopy  
266x188mm (72 x 72 DPI)



[A] Absorption and [B] emission spectra of RIVFF peptide obtained using UV-Visible spectrophotometry and fluorescence spectroscopy respectively  
341x98mm (72 x 72 DPI)

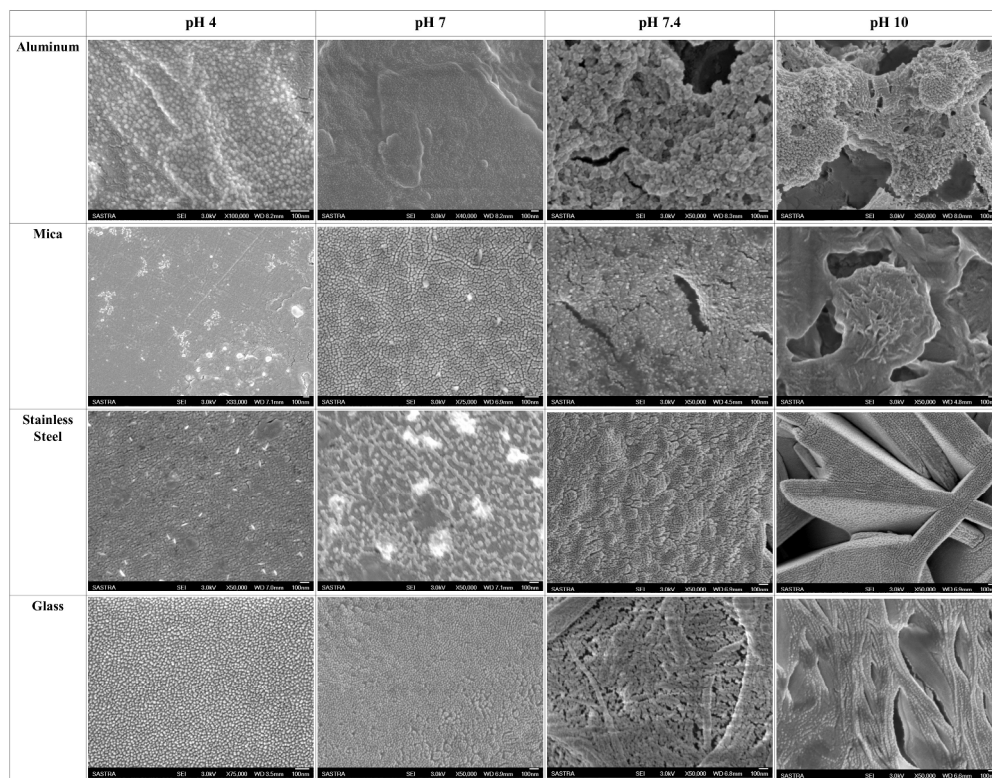
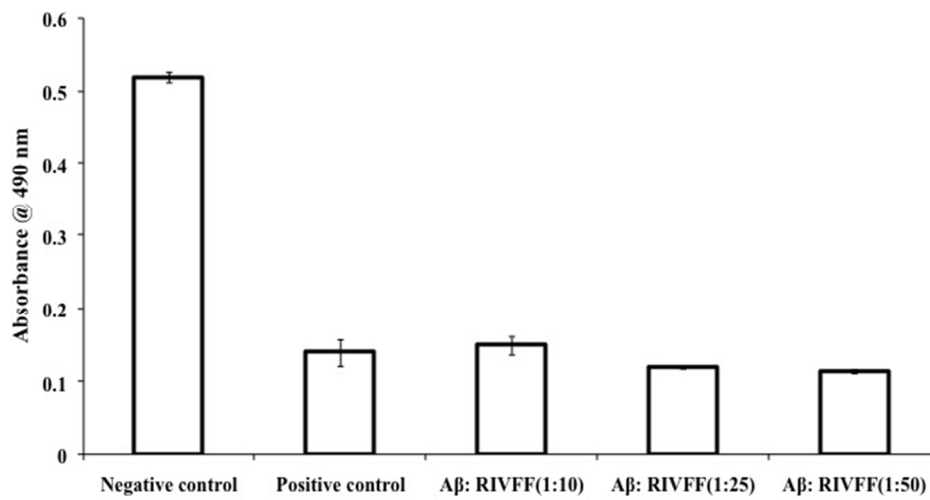


Figure 7: Scanning electron micrographs of self-assembled structure formed by RIVFF on various substrates namely stainless steel, mica, aluminum and glass at different pH

1136x882mm (72 x 72 DPI)



Cell viability of neuroblastoma cells exposed to different concentration of peptide in the presence of Aβ1-42  
253x132mm (72 x 72 DPI)